J. Mt. Sci. (2020) 17(4): 838-850 e-mail: jms@imde.ac.cn http://jms.imde.ac.cn
https://doi.org/10.1007/s11629-019-5688-0

Neotectonics of the Avaj region (NW Iran): left-lateral strike-slip and range-parallel reverse faults

Reza ALIPOOR* https://orcid.org/0000-0003-0596-6296; e-mail: rezaalipoor116@gmail.com

Amir Hossein SADR https://orcid.org/0000-0001-6705-0860; e-mail: Sadr_struct@yahoo.com

Sahar GHAMARIAN https://orcid.org/0000-0002-8678-2263; e-mail: ssghamarian@gmail.com

Geology Department, Faculty of Basic Science, Bu-Ali Sina University, Hamedan 009881, Iran

Citation: Alipoor R, Sadr AH, Ghamarian S (2020) Neotectonics of the Avaj region (NW Iran): left-lateral strike-slip and range-parallel reverse faults. Journal of Mountain Science 17(4). https://doi.org/10.1007/s11629-019-5688-0

Abstract: The aim of this study is the geomorphological analysis of neotectonic deformation in the Avaj region in the NW part of the Iranian Plateau. We use observations from detailed field surveys and the analysis of digital elevation model (DEM) and satellite images (Landsat-7 ETM+, 30-m resolution) to explore a new E-W trending strike-slip fault system in the study area. The major active faults of the Avaj region are the NW-SE trending Avaj and Hassanabad fault zones. The Avaj Fault is a SW-dipping reverse fault with a transport toward NE and the Hassanabad Fault is a NE-dipping reverse fault that has moved Paleozoic rocks over Cenozoic sedimentary units. Moreover, there are some E-W trending left-lateral strike-slip faults which cut Late Quaternary deposits. The relationship between the NW-SE and E-W faults indicates that the slip at the termination of the NW-SE faults changes from reverse to left-lateral strike-slip faults. The activity of the left-lateral faults has formed a series of offsets and displacements in drainage paths. These left-lateral faults probably initiated in 5±2 Ma because of the convergence between the Central Iran and the South Caspian blocks.

Keywords: Active tectonic; Offset; Earthquake; Geomorphology; Avaj Fault; South Caspian

Received: 11-Jul-2019
1st Revision: 18-Sep-2019
2nd Revision: 16-Dec-2019
Accepted: 27-Feb-2020

Introduction

Many destructive earthquakes have occurred during the past centuries in NW of the Iranian Plateau (Stöcklin et al. 1968; Berberian and King 1981). The present-day convergence between the Arabian and Eurasian plates and the motion of the South Caspian and Central Iran blocks are responsible for these destructive earthquakes (Berberian 1983; Axen et al. 2001). The southern Caspian block is moving to the northwest and the Central Iran is moving to the east due to this convergence (Priestley et al. 1994). Generally, the seismicity and dominant tectonic features of the boundary between these blocks in NW Iran involve reverse faults (Coplay and Jackson 2006; Ritz et al. 2006; Toori and Seyitoglu 2014).

The Avaj region in NW Iran is located in a critical area among these major reverse faults and the active tectonic belt between the Central Iran and the Caspian blocks constitutes the morphology of this region (Figure 1). Although earthquakes with the magnitudes of up to 6.5 (Changureh-Avaj earthquake (MW=6.5) on June 22, 2002) have occurred in the Avaj region, there is no detailed geological study on the active faults of this region. Most previous studies focused on the focal mechanism, epicenter location, and source parameters of the Changureh-Avaj earthquake (i.e,

Zare 2003; Gheitanchi 2004; Walker et al. 2005). Therefore, the current study has focused on the geometrical and kinematic analyses of the active faults of this region. We present a new interpretation for active faults of the Avaj region and propose a new E-W trending left-lateral strike-slip fault system in addition to the NW-SE trending reverse faults mentioned in previous studies. For this purpose, detailed field observations and the analyses of satellite images and digital elevation models are used.

1 Geological Setting

The Avaj region is located in the collision zone between the Arabian and Eurasian plates at the NW end of the Central Iran geological zone (Figure 1). This region corresponds to two different geological subzones based on surface outcrops: the Abegarm sub-zone in the NE and the Razan sub-zone in the SW (Bolourchi 1979) (Figure 2). The boundary between these two sub-zones is coincident with the NW-SE trending Avaj fault zone. In the Razan sub-zone, the Paleozoic and Lower to Middle Triassic depositions are not exposed and the oldest formations are the slightly metamorphosed rocks of upper Triassic-Jurassic strata which are disconformably overlain by upper Jurassic conglomerate and limestone. The Tertiary rocks of the Razan sub-zone compose a relatively complete succession. The Abegarm sub-zone is located in the NE part of the study area, is composed of a relatively complete succession of Precambrian (i.e. the Kahar Formation) to recent deposits, and comprises several unconformities and gaps. (Bolourchi 1979). The NE part of this sub-zone has been dissected by the Hassanabad and Kharrud faults. Furthermore, the most important fault structures around the Avaj region are the E-W trending Ipak fault zone, the NW-SE trending Soltanieh fault zone, and the WNW-ESE trending Koushke-Nosrat fault zone (Berberian 1983; Allen et al. 2011).

2 Material and Methods

In this paper, we propose geometrical and kinematical evidence of new E-W trending left-lateral strike-slip fault systems in the Avaj region based on three types of data: digital elevation model, geological maps, and field data. First, the analyses of the satellite images (Landsat-7 ETM+, 30-m resolution) and the digital elevation model indicate a neotectonic evidence of fault movements such as offsets along the path of streams. These offsets were calculated by projecting the trend of

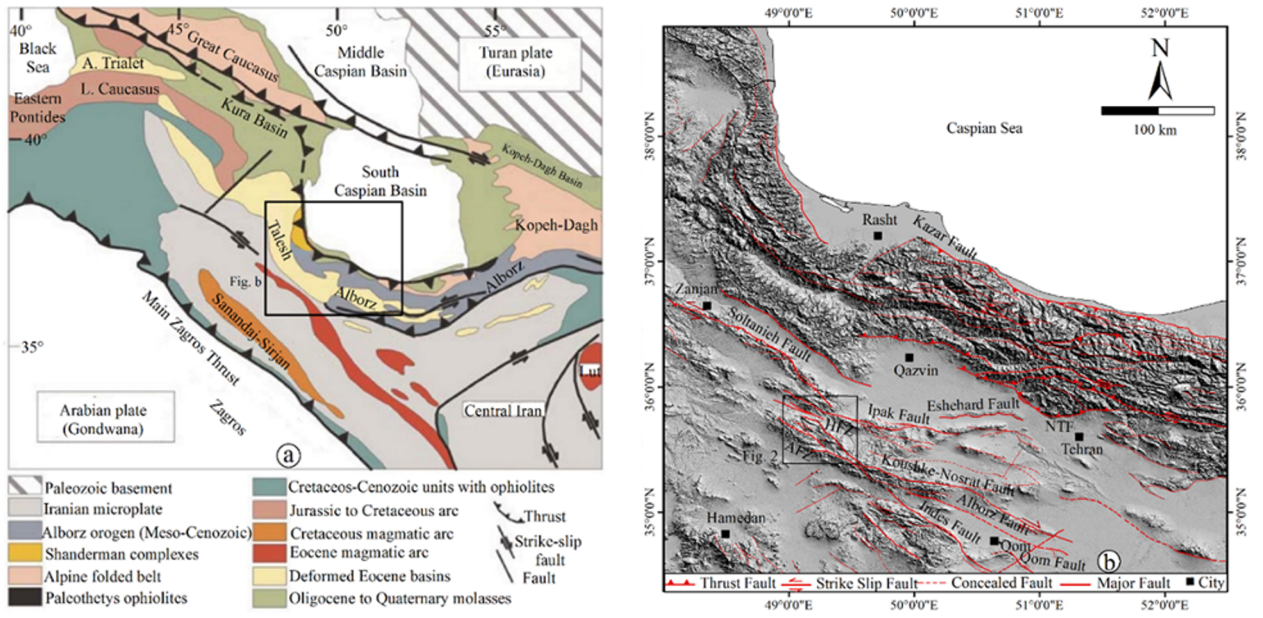

Figure 1 (a) General tectonic setting of the north Iranian Plateau (Zanchetta et al. 2009). The black rectangle shows Figure 1b. (b) General tectonic map of the north Iranian Plateau merged with the SRTM image. The black rectangle shows the location of the study area. AFZ: Avaj fault zone, HFZ: Hassanabad fault zone, NTF: North Tehran Fault.

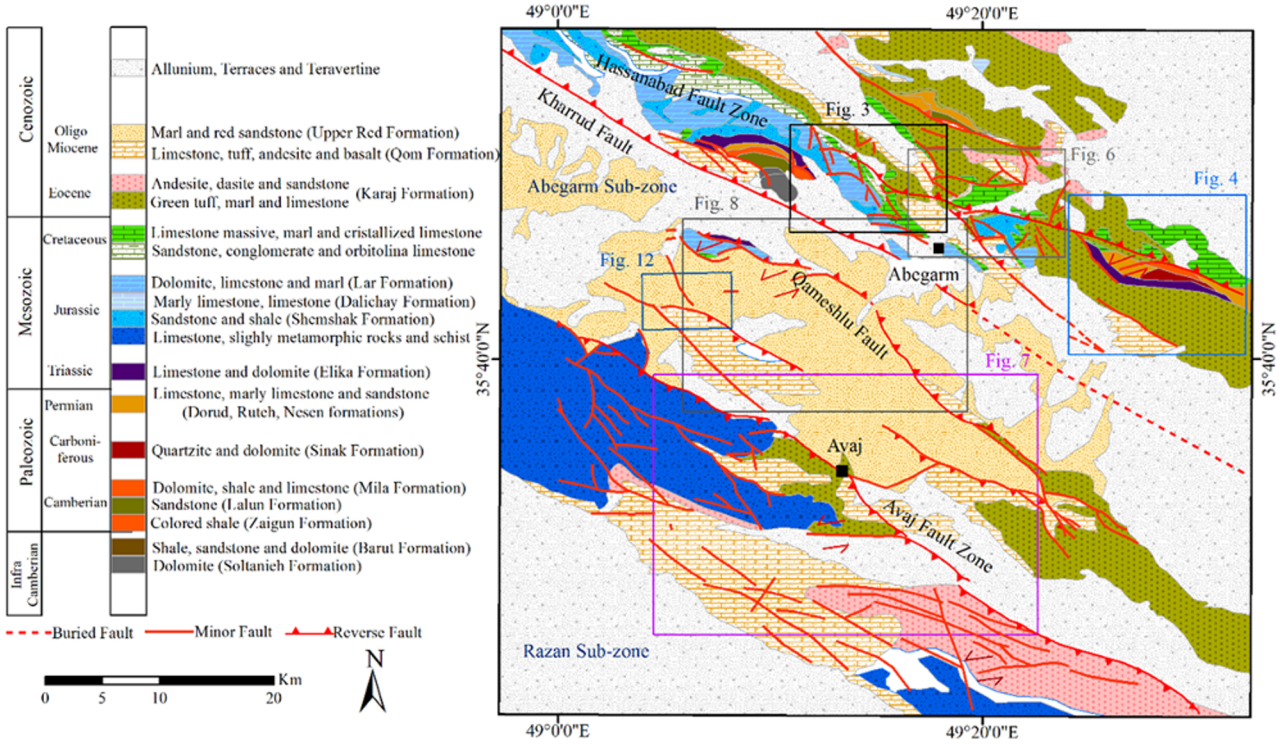

Figure 2 The geological map of the study area (Bolourchi 1979). The Razan and Abegarm sub-zones are located in the southeast and northeast of the study area, respectively. The rectangles show the locations of the following figures.

the downstream and upstream sections to the fault trend and the distance between the projected points indicates the amount of the offsets (Alipoor et al. 2012; Yan and Lin 2015). The digital elevation model was obtained by ArcGIS from Shuttle Radar Topography Mission (SRTM, 30-m resolution). Geological maps at 1/1.000.000 scale (Bolourchi 1979) and high-resolution Google Earth images provided information about the lithologies, faults trends, and major landforms of the study area. Then, we examined the results of the E-W left-lateral faulting through field observations. The evidence of faulting in the field observations included the slickenline on fault planes, displacement in layers, faults breccia, and fault steps.

3 Results and Interpretations

The morphology of the Avaj region is composed of two NW-SE trending ranges and sub-basins (the Abegarm and Razan) (Figure 2). In previous studies, the regional morphology was explained by the NW-SE trending reverse faults and new observations presented in this research demonstrate new E-W trending left-lateral strike-slip faults. Generally, the active fault zones in the Avaj region are divided into two major NW-SE trending fault zones, namely, the Hassanabad fault zone in the northern part and the Avaj fault zone in the central and southern parts (Figure 2). The E-W trending left-lateral strike-slip faults have formed between the NW-SE faults segments and the slip at the termination of the NW-SE faults changes from reverse to left-lateral strike-slip mechanism. In addition, the recent activity of the left-lateral faults has formed a series of offsets and displacements in the drainage paths. However, our findings in this paper present a new description of the neotectonic framework for the Avaj region.

3.1 Hassanabad fault zone

The Hassanabad fault zone is located in the northern part of the Avaj region and the most important structures in this zone are NW-SE trending Hassanabad and Kharrud reverse faults. The NW-SE trending Hassanabad Fault with a length of about 75 km is exposed in the northern part of the Abegarm sub-zone. The eastern termination of this fault extends to the Ipak seismic

fault (Fig. 1). Noticeably, the Ipak Fault has been disrupted during the Buin-Zahra earthquake of September 1, 1962 (Ms=7.2) (Ambraseys and Melville 1982) with a reverse dip separation of about 1.4 m and a left-lateral strike-slip displacement of 0.6 m (Berberian 1983).

Although the Hassanabad Fault had previously been mapped in the geological map of the study area (Bolourchi, 1979), there is no data about the kinematics and geometry of this fault. Our findings indicate two sets of fault planes with different kinematics in the Hassanabad fault zone. The first set comprises the NW-SE trending reverse faults which moved Paleozoic rocks over Cenozoic sedimentary units. The second set is composed of the recent E-W trending strike-slip faults cutting Cenozoic rocks and Quaternary alluvium (Figure 2). The NE-dipping Hassanabad reverse fault is the most prominent NW-SE structure (Figure 3a) which has transported the middle Cretaceous limestone over the upper Cretaceous limestone and marls. In the vicinity of the Aghche-Qaleh village, the Hassanabad fault plane is well exposed (Figure 3b) with an attitude of N55°W/85°NE (Figure 3c). Accordingly, the mechanism of this fault is a NE-dipping reverse fault and the direction of the fault plane lineation indicates a transport toward SW (Figure 3d). Indeed, the sensation of roughness is in the direction of fault movement. The NW-SE trending Kharrud reverse fault with a length of more than 40 km is another important fault in the central part of the Abegarm sub-zone (Figure 3). Cambrian to Mesozoic deposits are exposed in the northern part of this fault, whereas there is a depression basin in the southern part. This fault separates the lower Paleozoic deposits in the northeast from the Cenozoic deposits in the southwest.

The NE-dipping reverse Hassanabad Fault and other left-lateral strike-slip faults are observable at several localities. Both left-lateral strike-slip and reverse fault planes are exposed near Sinak and Hassanabad villages (Figure 4a). Close to Sinak village, the massive limestone of the upper

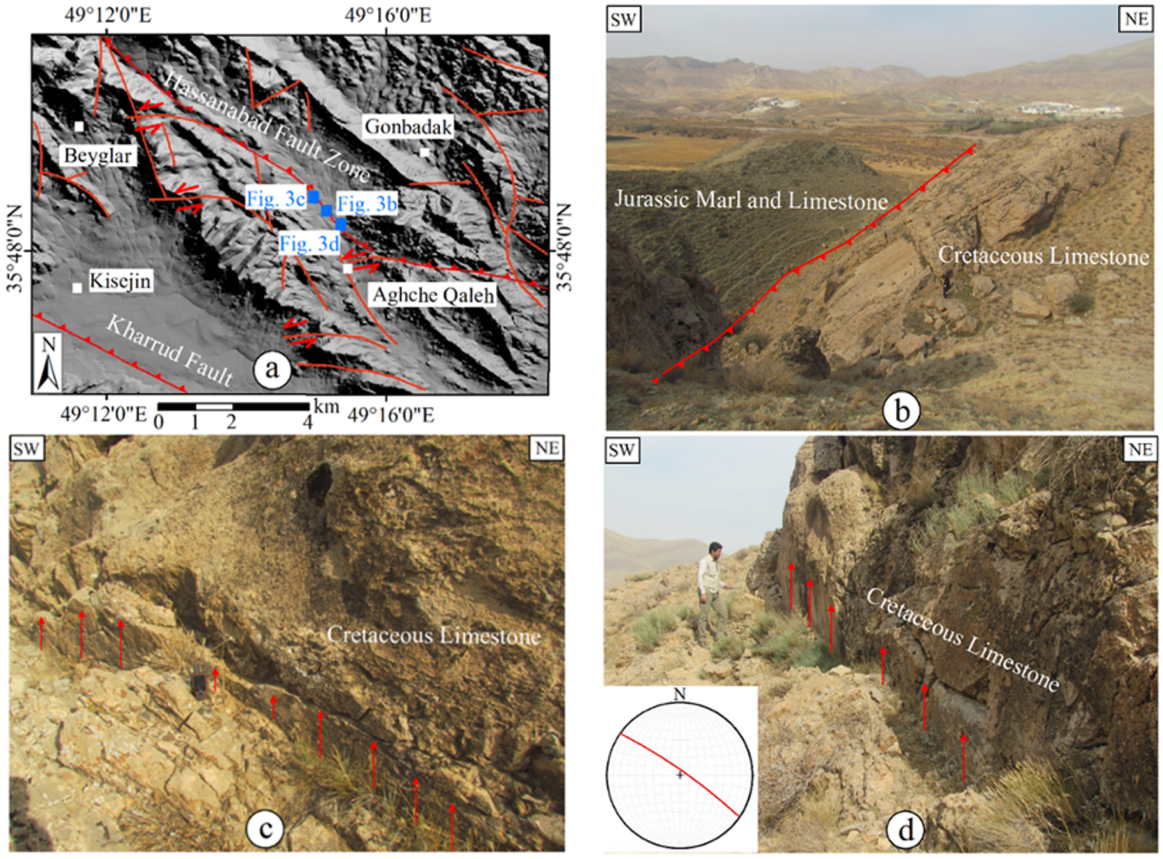

Figure 3 (a) SRTM image map of the Hassanabad fault zone. See Figure 2 for the location. The blue box shows the location of Figures 3b, 3c, and 3d. (b) Cretaceous limestones are thrust over the Jurassic marl and limestone along the Hassanabad fault zone. (c), (d) The fault plane of the Hassanabad Fault with a NW-SE trend.

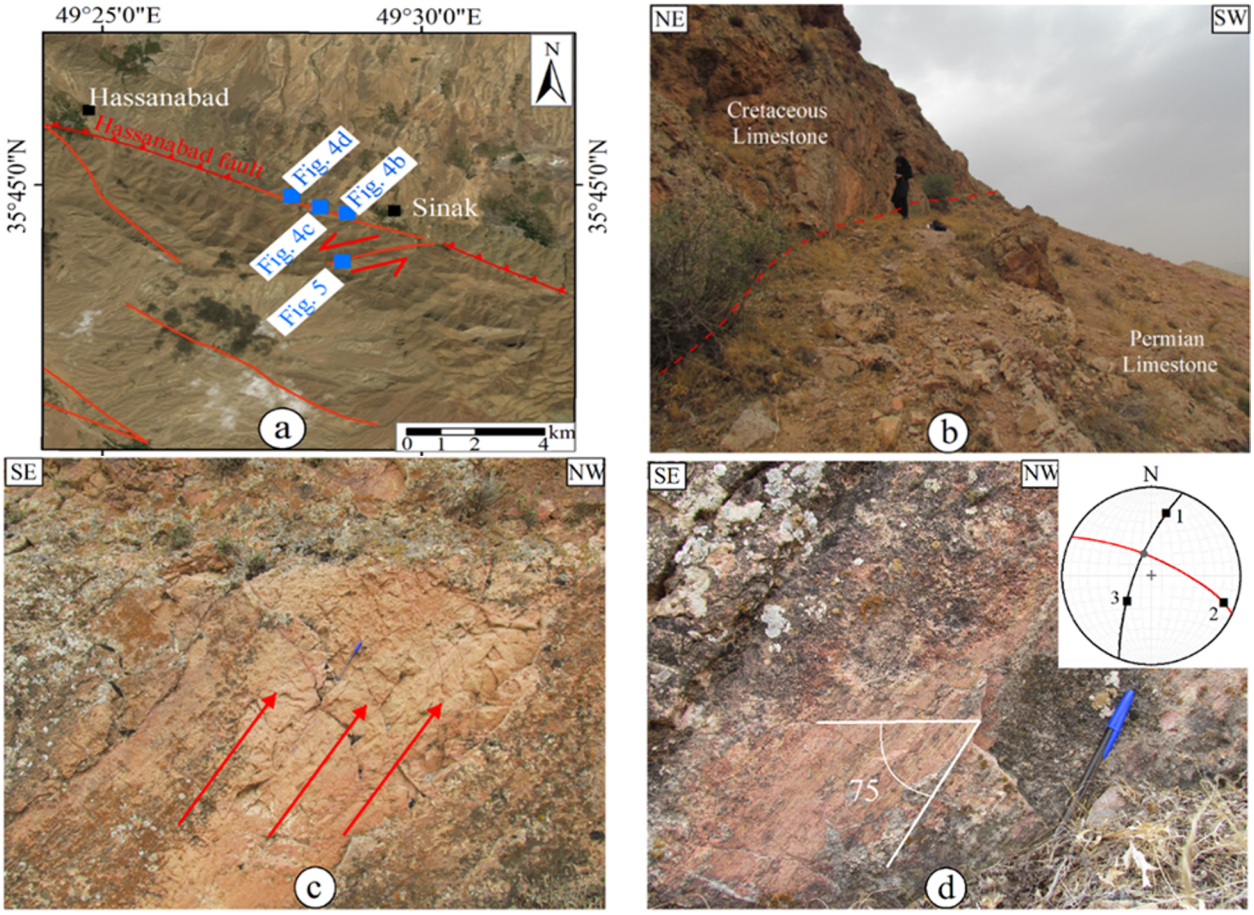

Figure 4 (a) Google Earth image of the SE part of the Hassanabad fault zone. See Figure 2 for the location. (b) The Hassanabad fault zone causing the thrusting of the Cretaceous limestone over the Permian limestone. (c) The Hassanabad fault plane surface, and (d) slickenline on the fault plane with a slip rake angle of 75°S indicates a reverse mechanism.

Cretaceous was uplifted due to the movement of the Hassanabad Fault and emplaced over the Permian limestone and sandstone (Figure 4b, Figure 2). The striations on the fault plane surface demonstrate a reverse displacement in the fault zone and a transport toward the SW (Figure 4c). These striations indicate the left-lateral component of the oblique reverse slip on the Hassanabad Fault. The attitude of this fault plane is N65°W/75°NE with a slip rake angle of 75°S. This reverse fault has cut the Cretaceous limestone and the motion of the hanging-wall is upward and to the right (left-lateral oblique) as evidenced by the slickenlines and steps on the fault plane (Figure 4d).

The Hassanabad and Kharrud reverse faults are the oldest faults of the study area continued by E-W left-lateral strike-slip faults. A number of left-lateral strike-slip faults are observed in the Hassanabad fault zone. Close to Sinak village, a fault plane with a strike-slip mechanism cuts the Permian limestone (Figure 5a). The attitude of this fault plane is N80°E/85°NW with a slip rake angle of 20°S (Figure 5b). The striations and nearly horizontal slickenlines on this fault plane indicate a left-lateral strike-slip mechanism. Thus, two fault plane sets were recognized in the Hassanabad fault zone: early reverse faults (Figure 3 and 4) and late left-lateral strike-slip faults (Figure 5). The data obtained from the NW-SE reverse faults and E-W left-lateral strike-slip faults indicate that the slip at the termination of the NW-SE faults changes from reverse to left-lateral strike-slip in the study area (Figures 5 and 6).

The E-W trending left-lateral strike-slip faults are also observed in the middle parts of the Hassanabad fault zone (Figure 6a). Close to Qaleh Abdollahkhan village, limestone and marl of Eocene are cut by a vertical E-W trending fault

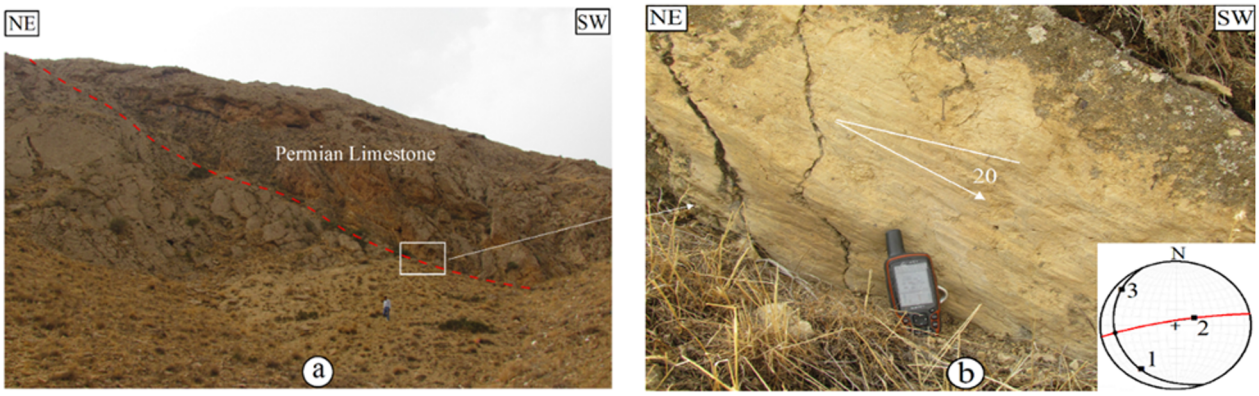

Figure 5 (a) Permian limestones have been displaced by an E-W trending strike-slip fault along the Hassanabad fault zone. See Figure 4 for the location. (b) The nearly horizontal slickenlines (with a slip rake angle of 20°S) on the fault plane surface indicate left-lateral strike-slip movements.

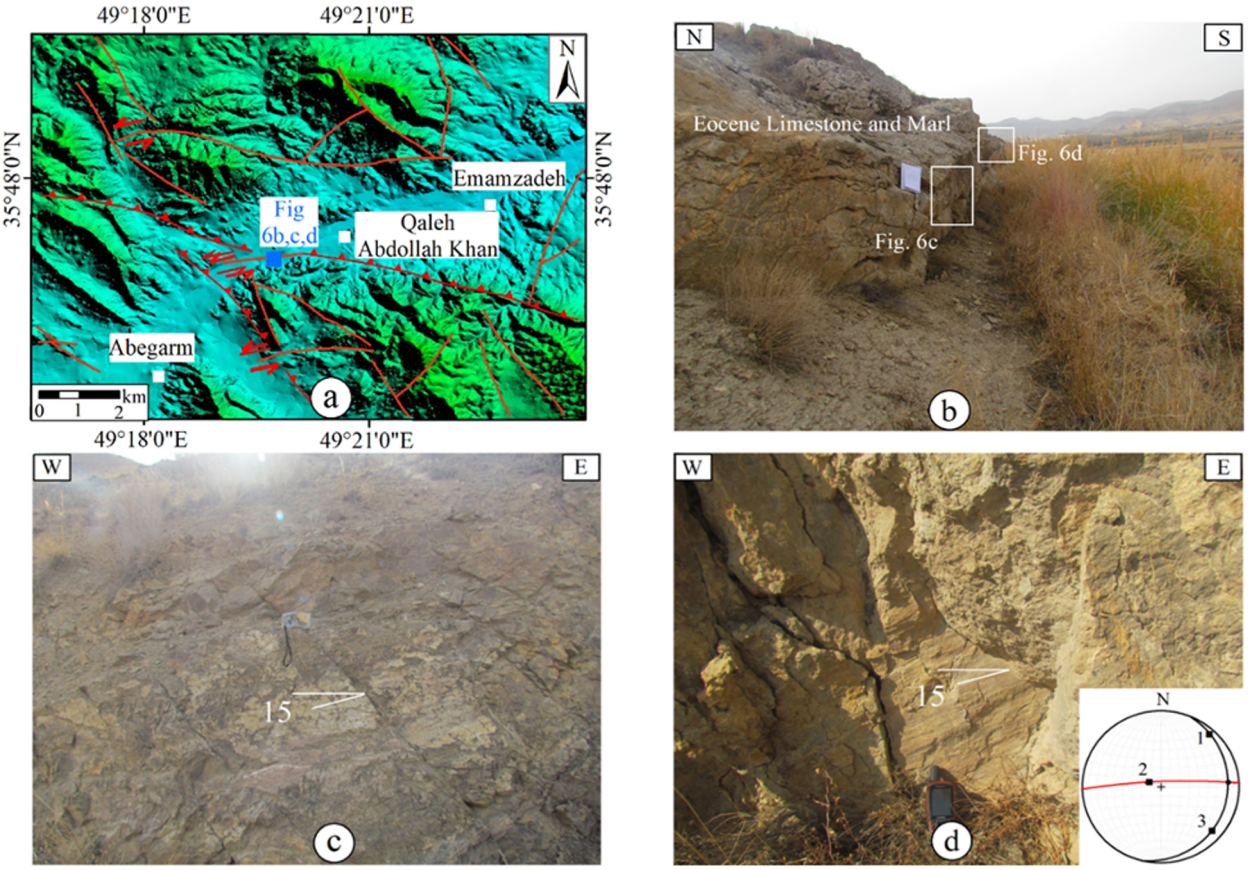

Figure 6 (a) The SRTM image of the middle part of the Hassanabad fault zone. See Figure 2 for the location. (b) The fault zone of the E-W trending strike-slip fault has cut Eocene limestone and marl. (c), (d) The fault plane surface and sub-horizontal slip rake angle (15°S) show a left-lateral strike-slip mechanism.

(Figure 6b). The indicators of this fault plane such as the nearly horizontal slickenlines indicate a left-lateral strike-slip movement (Figure 6c). The attitude of the fault plane is N88°E/85°NW with a slip rake angle of 15°S (Figure 6d). Hence, our structural field data from the Hassanabad fault zone demonstrate that two different fault mechanisms occur in the northern part of the study area. The NW-SE trending longitudinal faults are the main structures in the study area. The E-W trending left-lateral strike-slip faults comprise the recent range-crossing faults. This indicates that the mechanisms of reverse faults, at least at their termination, have changed into left-lateral strike-

slip faults.

3.2 Avaj fault zone

The Avaj fault zone with a length of about 75 km passes through Avaj city and separates the Abegarm and Razan sub-zones (Figure 7a). The strike of this fault varies from N50°W to N60°W in the boundary between the metamorphic rock units of the Razan sub-zone and recent alluvium deposits (Figure 1). The Avaj Fault has been reactivated since the Eocene and pyroclastic metamorphosed upper Triassic-Jurassic rocks were transported over the Miocene Upper Red Formation.

The Avaj reverse fault trace has been observed at several localities (Figure 7). The limestone, marl, and green tuff of the Karaj Formation (Eocene) in the southwest of Avaj city were uplifted due to the Avaj reverse fault and emplaced over the marl and red sandstone of the Upper Red Formation (Figure 7b). This oblique SW-dipping reverse fault has formed a crash zone. The fault plane indicators such as striations and nearly vertical slickenlines demonstrate a reverse displacement in the fault zone and a transport to the NE (Figure 7c). The attitude of this fault is N56°W/72°SW with a slip rake angle of 70°S (Figure 7d).

The NW-SE trending Qameshlu Fault is another prominent structure between Avaj and Abegarm cities. This fault begins near Qameshlu village and extends about 45 km toward the southeast (Figure 2). Limestone, tuff, and basalt of the Qom Formation (Oligo-Miocene in age) in the NE part of this fault were uplifted and emplaced over the marl and red sandstone of the Upper Red Formation (Figure 2). The Qameshlu reverse fault is observed at several localities (Figure 8a). Detailed field observations revealed that this fault trace is associated with two styles of faulting in the outcrop. The limestone of the Triassic Elika Formation has been thrust over the dolomite and limestone of the Jurassic Lar Formation in the northwest of Gandahu village (Figure 8a). The fault

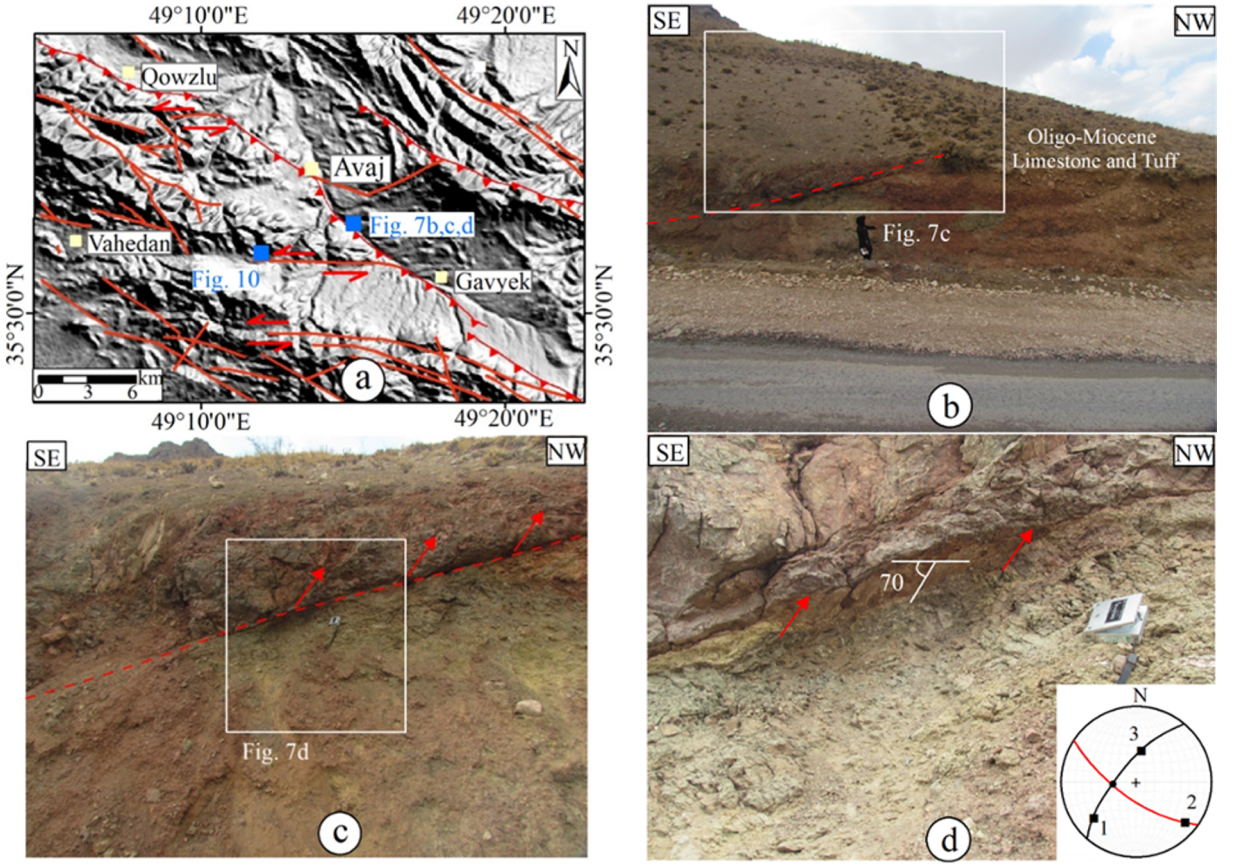

Figure 7 (a) The SRTM image shows the Avaj fault zone. See Figure 2 for the location. (b) The Avaj fault zone crosses the Oligo-Miocene limestone and marl. (c) The fault zone, and (d) the fault plane surface of the NW-SE reverse Avaj Fault with a slip rake angle of 70°S.

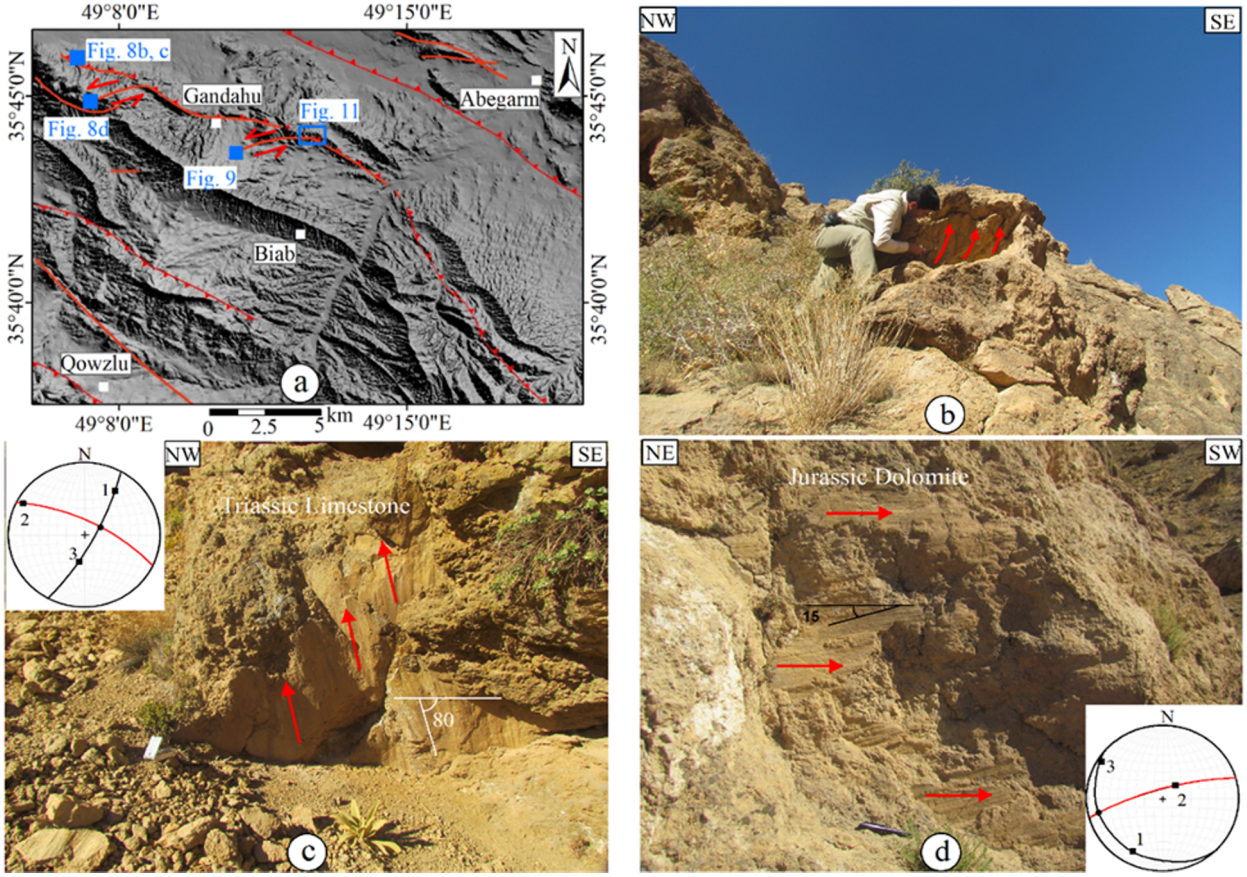

Figure 8 (a) The SRTM image of the Qameshlu fault zone. See Figure 2 for the location. The blue boxes show the locations of Figures 8b, 8c, and 8d. (b), (c) the fault plane surface and the nearly vertical slickenline (with a slip rake angle of 75°S) indicate the reverse mechanism of the Qameshlu Fault. (d) E-W left-lateral strike-slip faults crossing the Qameshlu reverse fault

plane indicators demonstrate a displacement toward the SW along this NE-dipping reverse fault (Figure 8b). The nearly vertical slickenlines indicate a reverse faulting in this part of the Qameshlu Fault (Figure 8c). The measured fault plane attitude is N64°E/75°NW with a slip rake angle of 80°S indicating an oblique reverse displacement (Figure 8c). Both reverse and left-lateral strike-slip fault planes of the Qameshlu Fault are exposed in the northwest of Gandahu village indicating an oblique reverse and left-lateral strike-slip faulting along the Qameshlu Fault (Figure 8a). The field observations indicate that this reverse faulting is followed by E-W trending left-lateral strike-slip faults. Close to Gandahu village, a sharp fault plane crosses the Jurassic limestone. The attitude of this fault is N76°E/80°NW with a slip rake angle of 15°S and the slickenlines on the fault plane indicate a left-lateral strike-slip faulting (Figure 8d).

Furthermore, left-lateral strike-slip faults along the Qameshlu Fault can be observed in the south of Gandahu village (Figure 8a). Marl and red sandstone of the Upper Red Formation are cut by strike-slip faults indicating recent left-lateral displacement (Figure 9a). High angle dip and nearly vertical bedding of the Upper Red Formation marl close to the Qameshlu fault zone are detectable in the field observations (Figure 9b). The fault responsible for this deformation through the variegated layers of the Upper Red Formation is a NE-dipping strike-slip fault. Structural and morphological evidence demonstrates a left-lateral shear along this fault. The attitude of this fault is N84°E/82°NW with a slip rake angle of 30°S. Striations and nearly horizontal slickenlines on the fault plane indicate the left-lateral strike-slip displacement of the fault (Figure 9c).

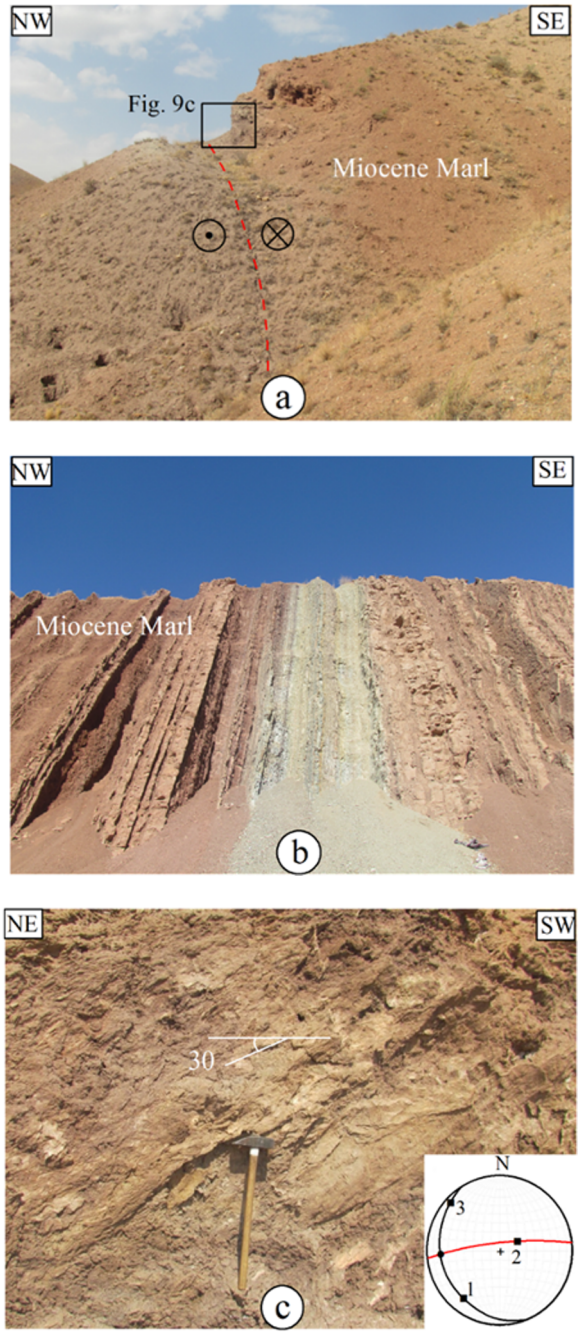

Figure 9 (a) A left-lateral strike-slip fault crosses the Miocene marl in the south of Gandahu village. See Figure 8 for the location. (b) The vertical bedding of the Miocene marl along the E-W trending strike-slip faults of the Qameshlu fault zone. (c) The nearly horizontal slickenline on the fault plane indicates left-lateral strike-slip movements.

At the middle part of the Avaj Fault, left-lateral strike-slip faults cut recent alluvium and terraces in the south of Avaj city (Figure 7). A prominent fault trace in the Quaternary alluvial deposits occurs near the termination of the E-W striking faults (Figure 10a). The deep incision on the valley floor due to the displacement of these strike-slip faults demonstrates a rapid vertical denudation (Figure 10b). In this part of the study area, the Quaternary alluvia are exposed along a linear, abrupt, topographic step caused by recent E-W strike-slip faults. The nearly horizontal slickenlines on this fault plane indicate its left-lateral strike-slip movement. The attitude of this fault is N90°E/85°S with a slip rake angle of 10°S (Figure 10c). Morphologically, the E-W striking left-lateral strike-slip faults in the Avaj fault zone continue the NW-SE trending major reverse faults.

3.3 Geomorphological evidence for left-lateral movements

The displacement of the drainage paths is a useful method for measuring fault offsets and has already been used in Iran (i.e. Talebian and Jackson 2002; Alipoor et al. 2012; Alipoor et al. 2011) and elsewhere (Wallace 1968; Replumaz et al. 2001). The examination of satellite images and aerial photos indicates a series of offsets and displacements in the drainage paths of the Avaj fault zone. The recent E-W trending left-lateral strike-slip faults of the Avaj region have affected the drainage paths and the amount of fault offsets can be estimated by restoring these drainage paths. Thus, in this study, the offsets along the drainage paths were measured based on the analyses of Landsat satellite images and digital elevation model.

The first offset along the left-lateral strike-slip fault was measured in the middle part of the Qameshlu fault zone (Figure 8). Google Earth images indicate a strike-slip fault trace near Qezel-Tappeh village where a left-lateral offset of about 850 m is detectable in the drainage path (Figure 11a). The amount of offset on this E-W trending left-lateral strike-slip fault could be estimated via the restoration of the drainage paths. Figure 11b indicates the fault before and after the 850 m restoration of the left-lateral strike-slip movements.

The strike - slip movement along the NW part of the Avaj fault zone has led to the deflection of the drainage paths. To estimate the amount of offset in this part of the study area, Google Earth images were used. A left-lateral offset along the E-W trend fault is visible near Shurab village (Figure

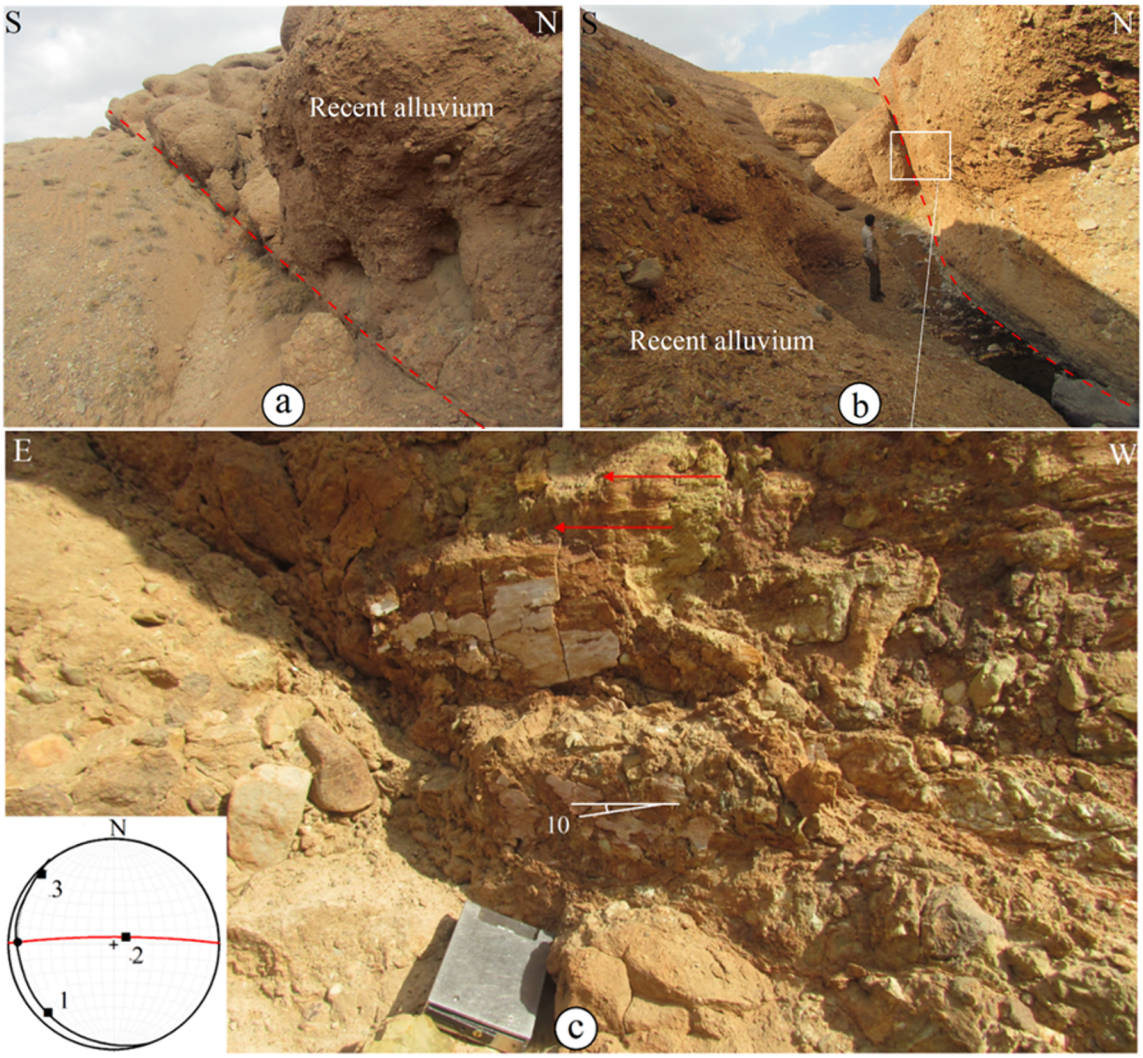

Figure 10 (a) and (b) Alluvial deposits are displaced by cross-cutting left-lateral strike-slip faulting along the Avaj fault zone. See Figure 7 for the location. (c) Slickenlines on the fault plane with the slip rake angle of 10°S show a left-lateral strike-slip mechanism.

12a). This left-lateral offset in the NW part of the Avaj fault zone has caused a displacement of about 2500 m (Figure 12b).

4 Discussion

The recent morphology of the Avaj region is due to the activity of the major active faults. These faults have been responsible for many destructive earthquakes and the Changureh-Avaj earthquake of June 22, 2002 is the most important instrumentally recorded earthquake in the Avaj region. This earthquake with an estimated magnitude of MW 6.5 occurred at 07:28 local time (02:58 GMT) in a sparsely populated region (Walker et al. 2005). The focal mechanism solution of this earthquake indicates a thrust fault and must be related to the Avaj thrust fault (Toori and Seyitoglu 2014) (Figure 13). Our findings in this research indicate two stages of faulting in the Avaj region in the NW of Iran. In the early stage, major NW-SE trending longitudinal reverse faults developed in response to the oblique convergence between the Arabian and Eurasian plates. In the late stage, E-W trending left-lateral strike-slip faults occurred during the partitioning of the deformations in the study area. It is suggested that the early stage was related to the Cretaceous oblique convergence, while the late stage resulted from the Cenozoic collision. Considering the recent movements and activities along the major fault

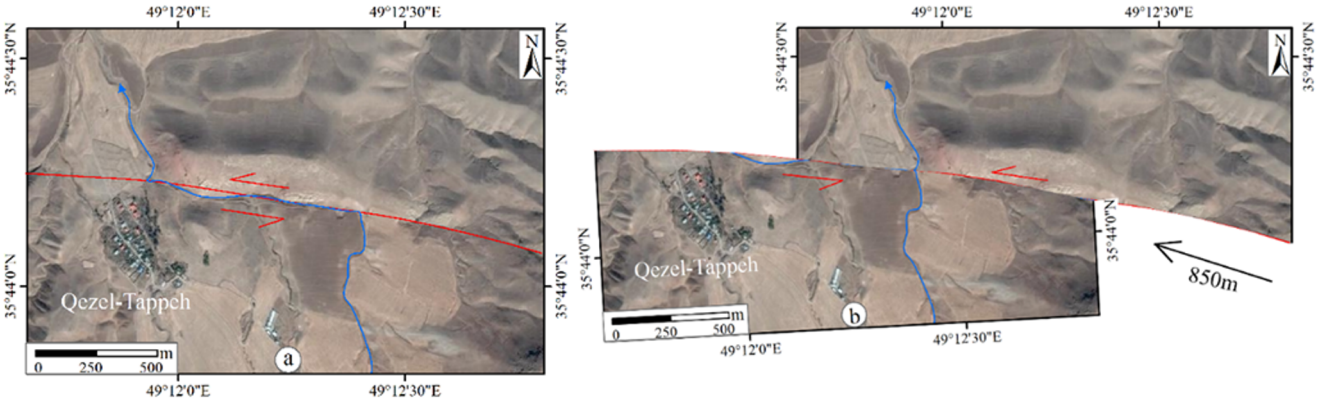

Figure 11 (a) and (b) Google Earth images of the left-lateral fault movement before and after the reconstruction of 850 m offset. See Figure 8 for the location. The locations of the fault and drainage paths are shown by red and blue lines, respectively.

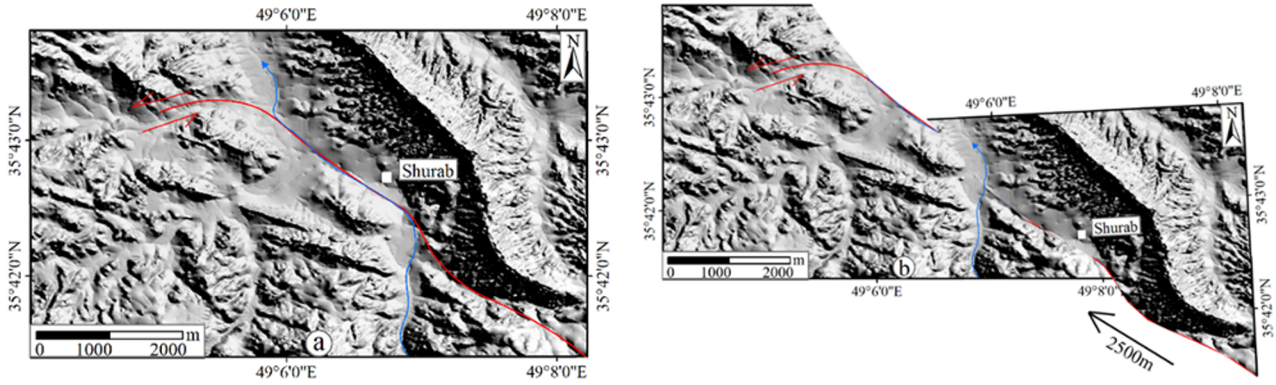

Figure 12 The SRTM image of the NW part of the Avaj fault zone before and after reconstructing the 2500 m left-lateral movement. See Figure 2 for the location. The symbols are identical to those of Figure 11.

zones of the study area, it is important to determine the precise timing of the inception of the left-lateral deformation. The recent morphology of the study area is controlled by the oblique plate movements between the Central Iran and South Caspian blocks. Generally, these oblique plate movements and the clockwise rotation of the South Caspian block caused a left-lateral shear in the Avaj region. Therefore, the left-lateral movements along the active fault zones of the Avaj region may have been initiated when the South Caspian block began to rotate.

Based on the observations of surface faulting and earthquake focal mechanisms, Jackson et al. (2002) suggested that the present motions of the South Caspian block may have begun in Pliocene (3–5 Ma). By dating on zircon, biotite, K-feldspar, and apatite samples, Axen et al. (2001) noted that the subsidence of the South Caspian block and the reversal of Alborz strike-slip from right-lateral to left-lateral faults began in 5±2 Ma. Using morphotectonics and structural analysis, Ritz et al. (2006) suggested that the clockwise rotation of the South Caspian block began in the Pliocene age.

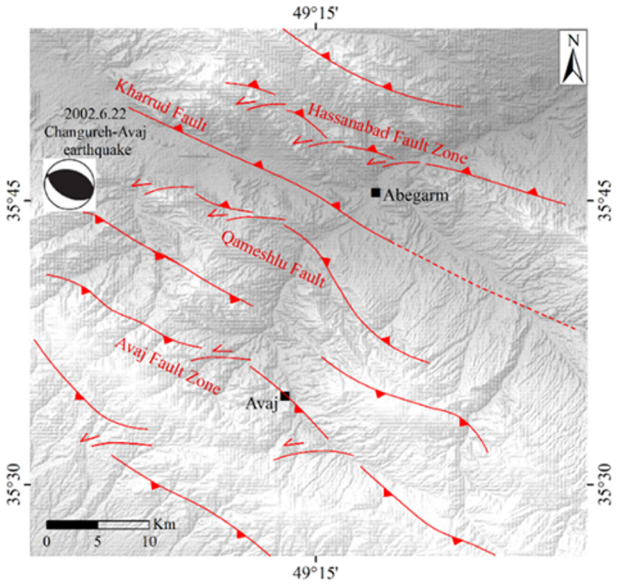

Figure 13 The SRTM image indicates a simplified neotectonic framework of the Avaj region based on the new structural data presented in this research.

Given that the oblique convergence between the Central Iran and South Caspian blocks caused a left-lateral shear, the left-lateral faulting in the Avaj region was probably initiated in 5±2 Ma.

The new data in this research indicate that the convergence between the Central Iran and South Caspian blocks has not been compensated only by the NW-SE trending reverse faults as described in previous studies. Rather, this convergence has also been compensated by E-W trending left-lateral strike-slip faults. The important point here is the relationship between NW-SE trending reverse faults and E-W trending left-lateral strike-slip faults in the study area. The major NW-SE trending reverse faults of the study area are the Kharrud and Hassanabad fault in the NE of the region and the Avaj fault zone in the SW part of the region. Thus, major longitudinal NW-SE trending fault zones of the study area indicate a reverse mechanism and the structural data presented in this paper demonstrate new E-W trending left-lateral strike-slip faults. These E-W trending left-lateral strike-slip faults in the Avaj region have been developed among the NW-SE trending reverse fault segments. Based on this new structural evidence, a new simplified neotectonic framework of the study area was constructed for the movements of the active faults and the description of the tectonic conditions in the study area (Figure 13).

5 Conclusion

The neotectonics of the Avaj region have been complicated by three active fault zones: the E-W trending Ipak fault zone with a left-lateral compression mechanism, the NW-SE trending Soltanieh fault zone with a left-lateral reverse mechanism, and the WNW-ESE trending Koushke-Nosrat Fault with a reverse mechanism and a left-lateral component.

The fault plane indicators demonstrate a reverse displacement and a transport to the NE in SW-dipping Avaj fault zone. The maximum offset along the E-W trending left-lateral strike-slip fault in this fault zone is about 2500 m. The Hassanabad and Kharrud fault zones are exposed in the NW termination of the Ipak fault zone. The fault plane geometry indicates that the Hassanabad Fault is an NE-dipping reverse fault with a left-lateral component.

The Avaj region is an active seismic zone and its neotectonics are controlled by the NW-SE trending range-parallel reverse faults and E-W trending range-crossing left-lateral strike-slip faults.

Oblique plate movements between the South Caspian and Central Iran blocks caused a left-lateral shear along the E-W trending strike-slip faults in the Avaj region. This left-lateral shear may have been initiated as the rotation of the South Caspian block began. Hence, it is proposed that the left-lateral movement in the study area may have been initiated in 5±2 Ma. Considering the damages to the buildings and structures and the surface ruptures caused by the 2002 Changureh-Avaj earthquake, it can be concluded that the study area is a seismically hazardous region.

Acknowledgments

The authors would like to thank H. Mohseni who made an editorial revision of the original draft of the manuscript. We also thank Arash Moradi for editorial assistance.

References

Alipoor R, Poorkermani M, Zare M, El Hamdouni R (2011) Active tectonic assessment around Rudbar Lorestan dam site, High Zagros Belt (SW of Iran). Geomorphology 128: 1–14. https://doi.org/10.1016/j.geomorph.2010.10.014

Alipoor R, Zare M, Ghassemi MR (2012) Inception of activity and slip rate on the Main Recent Fault of Zagros Mountains, Iran. Geomorphology 175–176: 86–97. https://doi.org/10.1016/j.geomorph.2012.06.025

Allen MB, Kheirkhah M, Emami MH, Jones SJ (2011) Right-lateral shear across Iran and kinematic change in the Arabia–Eurasia collision zone. Geophysical Journal International 184: 555–574. https://doi.org/10.1111/j.1365-246X.2010.04874.x

Ambraseys NN, Melville CP (1982) A History of Persian Earthquakes, Cambridge Earth Science Series. Cambridge University Press, London. p 212. https://www.amazon.com/History-Persian-Earthquakes-Cambridge-Science/dp/0521021871

Axen GJ, Lam PJ, Grove M, et al. (2001) Exhumation of the west central Alborz Mountains, Iran, Caspian subsidence, and collision related tectonics. Geology 29: 559–562. https://resolver.caltech.edu/CaltechAUTHORS:20130820-131207518

Berberian M (1983) The southern Caspian: a compressional depression floored by a trapped, modified oceanic crust. Canadian Journal of Earth Sciences 20: 163–183. https://doi.org/10.1139/e83-015

Berberian M, King GCP (1981) Towards a paleogeography and tectonic evaluation of Iran. Canadian Journal of Earth

Sciences 18: 210–265. https://doi.org/10.1139/e81-019
Bolourchi MH (1979) Geological Quadrangle Map of the KabudarAhang (Scale 1:250,000). Geological Survey of Iran, Tehran.
Coplay A, Jackson J (2006) Active tectonics of the Turkish–Iranian Plateau. Tectonics, 25, TC6006. https://doi.org/10.1029/2005TC001906
Gheitanchi MR (2004) The June 22nd 2002 Changureh–Avaj earthquake in Qazvin province, north central Iran. Journal of Earth and Space Physics 30: 23–30. https://doi.org/10.1111/j.1365-246X.2005.02516.x
Jackson J, Priestley K, Allen M, Berberian M (2002) Active tectonics of the South Caspian Basin. Geophysical Journal International 148: 214–245. https://doi.org/10.1046/j.1365-246X.2002.01588.x
Priestley KF, Baker C, Jackson J (1994) Implications of earthquake focal mechanism data for the active tectonics of the south Caspian basin and surrounding regions. Geophysical Journal International 118: 111–141. https://doi.org/10.1111/j.1365-246X.1994.tb04679.x
Replumaz A, Lacassin R, Tapponnier P, Leloup PH (2001) Large river offsets and Plio-Quaternary dextral slip rate on the Red River fault (Yunnan, China). Journal of Geophysical Research 106: 819–836. https://doi.org/10.1029/2000JB900135
Ritz JF, Nazari H, Salamati R, et al. (2006) Active transtension inside Central Alborz: a new insight into the northern Iran–southern Caspian geodynamics. Geology 34: 477–480. https://doi.org/10.1130/G22319.1
Stöclin J (1968) Structural history and tectonics of Iran: a review. American Association of Petroleum Geology Bulletin 52: 1229-1258. https://doi.org/10.1306/5D25C4A5-16C1-11D7-8645000102C1865D
Talebian M, Jackson J (2002) Offset on the main recent fault of NW Iran and implications on the late Cenozoic tectonics of the Arabia–Eurasia collision zone. Geophysical Journal International 150: 422–439. https://doi.org/10.1046/j.1365-246X.2002.01711.x
Toori M, Seyitoglu G (2014) Neotectonics of the Zanjan–Kazvin area, Central Iran: Left lateral strike slip induced. Turkish Journal of Earth Sciences 23: 260–276. https://doi.org/10.3906/kim-1210-57
Walker RT, Bergman E, Jackson J, et al. (2005) The 2002 June 22 Changureh (Avaj) earthquake in Qazvin province, northwest Iran: epicentral relocation, source parameters, surface deformation and geomorphology. Geophysical Journal International 160: 707–720. https://doi.org/10.1111/j.1365-246X.2005.02516.x
Wallace RE (1968) Notes on stream channels offset by the San Andreas Fault, Southern Coast Ranges, California. Geological Sciences Stanford University Publications 11: 6–20. http://activetectonics.asu.edu/ActiveFaultingSeminar/Papers/Wallace_1968_Stream_Channels_Offset.pdf
Yan B, Lin A (2015) Systematic deflection and offset of the Yangtze River drainage system along the strike-slip Ganzi-Yushu-Xianshuihe Fault Zone, Tibetan Plateau. Journal of Geodynamics 87: 13–25. https://doi.org/10.1016/j.jog.2015.03.002
Zanchetta S, Zanchi A, Villa IM, et al. (2009) The Shanderman eclogites: A late Carboniferous high-pressure event in the NW Talesh Mountains (NW Iran). Geological Society of London, Special Publications 312: 57–78. https://doi.org/10.1144/SP312.4
Zare M (2003) Seismotectonic of south Ghazvin plain and stress situation in the Buin-Zahra 1962 and Changureh 2002 Earthquakes prone areas. Proceedings of the 4th International Conference of Earthquake Engineering and Seismology, 2003, Tehran, Abstracts No.213. p 1596. https://www.civilica.com/Paper-SEE04-SEE04_ST11.html